Indirect Communication Between Non-Markovian Baths.

Ben S. Humphries,[1] Dale Green,[1] and Garth A. Jones[1, a)]
Faculty of Science, University of East Anglia, Norwich Research Park, Norwich, NR4 7TJ, UK

In this work we show that information transfer occurs between two baths, even in the absence of a direct coupling between the baths. This bath-system-bath-mediated information transfer leads to intricate non-Markovian dynamics in the open system considered. We show this through the development of a model for an undamped vibration in the presence of an overdamped bath. This two-bath model involves a new derivation of the hierarchical equations of motion (HEOM) for an overdamped Lorentz-Drude (LD) environment that is summed together with an undamped oscillator (UO) bath, termed LDUO-HEOM. The model is analysed using expectation values of the bath coordinates which demonstrates an approach to understanding dissipation and relaxation between multiple, coupled baths. The model generates 2D electronic spectra that are in qualitative agreement with single-bath models while eliminating additional superfluous damping, which was introduced by the finite spectral width of the under- damped bath in our previous two-bath underdamped-overdamped, 'bath vibration model' [*J. Chem. Phys.* 156, 084103 (2022)].

Keywords: non-Markovian, HEOM, undamped spectral density, overdamped spectral density, 2D spectroscopy, Lorentz-Drude

I. INTRODUCTION

Non-Markovianity in an open quantum system is characterized by the recurrence of information from the bath, back into the system. It has been hypothesized that non-Markovianity could be exploited as a quantum resource[1,2]. An interesting question is: how does information dynamics behave in open systems with multiple baths[3]? This question is relevant to a number of applications including quantum heat engines and quantum refrigerators. [3–10]

When considering this question, the construction of the open quantum system, and nature of the baths directly affects the information dynamics. In this work we consider a two bath open system comprising an undamped bath and an overdamped bath, where the baths are combined via a direct sum. As we will show, information exchange between the baths does occur despite the baths not being mixed via a tensor product. In essence, the system acts as an agent for transferring information between the baths via what we refer to as a bath-system-bath coupling.

In this work we use hierarchical equations of motion (HEOM) which are an important tool for modelling non-Markovian processes in a wide variety of applications including, but not restricted to, energy transduction, quantum information and quantum thermodynamics. While HEOM is incredibility powerful in its application and versatility, new equations must be derived from first principles for each new formulation. In recent years, there have been a number of new forms of HEOM[11] derived for specific cases including arbitrary spectral density (ASD) HEOM[12], dissipation equations of motion (DEOM)[13], and generalisations of HEOM[14–16]. These new derivations introduce additional flexibility into the decomposition of the Matsubara basis and hence account for different environmental structures. Further, the definition of the system-bath boundary has been demonstrated to have a profound impact on the dynamics of the OQS model [17–21]. This current work was motivated by some of our previous work where we considered system boundary placement by examining two different OQS models applied to a molecular system, where a vibrational mode is coupled to the electronic degrees of freedom. The models are called the Hamiltonian vibration model (HVM) and the bath vibration model (BVM). [22] In the HVM the intramolecular vibration is defined explicitly in the Hamiltonian and in the BVM the same vibration is removed from the Hamiltonian and subsumed into the bath via a canonical transformation. In practice, the BVM was constructed by combining an underdamped bath *added* to an overdamped bath, where the former describes the molecular vibrations and the latter the rest of the environment. In principle the HVM and BVM should be mathematically equivalent however we showed this was not the case in practice. This is because the in the case of the BVM, the additional bath gives rise to additional spectral broadening, that leads to superfluous damping that is not consistent with HVM dynamics and its resulting spectra. Our new derivation removes the spurious damping, without the computational expense of the ASD-HEOM. This is achieved through construction of a HEOM with two spectral density components, one overdamped (with a Lorentz-Drude form), and the other a completely undamped mode describing the pure intramolecular vibration. The derivation follows well established methods of Tanimura and co-workers[23–25]. As discussed in Humphries et. al.[22], the BVM results in intrinsic canonical damping from the underdamped mode, that we argued is superfluous when added to a second overdamped bath, which already describes the noisy environment. This originates from the canonical transform

a)Electronic mail: garth.jones@uea.ac.uk

which carries the underdamped vibration into the environmental degrees of freedom. By creating a hierarchy which contains an *undamped*, rather than underdamped, contribution we show that we can remove this artifact.

In Section II we outline key differences between one- and two-bath models, including a brief overview of some relevant, recent studies. In Section III we give a detailed account of the derivation of our LDUO model. In Section IV we briefly detail the parameters used in the simulations employing the LDUO model. In Section V we present our results which includes and analysis of the resulting 2D electronic spectra and a detailed analysis bof that bath dynamics through expectation values of collective bath coordinates, before conclusions in Section VI.

II. BACKGROUND AND APPROACH

Undamped hierarchies have been constructed in earlier works[26,27], where the stability of these models have been dramatically improved by some researchers[28]. Our work is a novel extension of these models through the addition of a second overdamped (Lorentz-Drude) bath to the undamped bath. This construction differs from previous works on canonically transformed, *underdamped*, equations because of how the environment is constructed. In works by Garg[29], Lai[30], Green[31], and Tanimura[23,32], a *pure* system vibrational mode is extracted from the Hamiltonian and placed via the canonical transform into a Markovian bath. This is shown schematically in Figure 1(a), where superimposing the pure harmonic frequency (described by a delta function) with a Markovian environment (described by white noise) results in an underdamped (i.e. Lorentzian) spectral density. In particular we note that this environment is described by a single bath. In such a model there is *no* superfluous canonical damping as the environment is correctly described by the white noise component of the single spectral density.

Now we require the environment to be described by an overdamped spectral density, rather than purely white noise. To do this we adopt a *two-bath approach* where the overdamped contributions are defined by a Lorentz-Drude spectral density. Importantly this means that the environment contributions will have some non-Markovian character, see Green et al. for more details[31]. Previous studies canonically subsumed a system vibration into an overdamped environment by combining a Lorentzian with an overdamped spectral density, through a two-bath model. However, as we showed with the BVM, by doing this environmental damping is over-represented by doubling up on the environmental noise, see Figure 1(b), because there is noise in the Lorentzian as well as the LD spectral density. In 2022 we showed that a two-bath model in the limit of zero canonical damping is equivalent to a single-bath approach[22]. This motivated the current work where we now seek to develop a new model whereby the vibration remains in the bath but the white noise component is removed entirely. This is combined

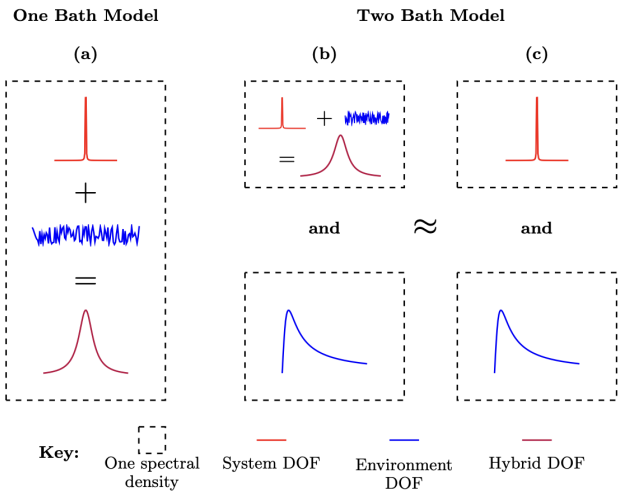

FIG. 1: Schematic of (a) *two component*, one bath model, (b) a *three component*, two bath model, and (c) the limiting case of (b) as a *two component*, two bath model.

with an overdamped, Lorentz-Drude, spectral density as part of the HEOM derivation, thereby removing the superfluous damping, as seen in Figure 1(c).

There are a number of motivational factors for doing this. Firstly it means that we can choose where to place the vibrational mode, the system Hamiltonian or the bath, which may have practical implications such as computing time. However, there is also significant theoretical interest, as it gives us insight into information dynamics between the bath and the system, which is an important area of study in open quantum systems. In particular in this work, we will investigate how information is exchanged between the two baths, via the quantum system. This is of general theoretical interest because non-Markovianity can be understood as a resource in quantum information theory. While a detailed analysis is outside the scope of the current work, this model has the potential to offer insight into how information might be fed between baths and back into a quantum system from its environment (recurrence).

III. MODEL AND DERIVATION

The one bath model consists of a one-dimensional system coupled to an overdamped bath of N harmonic oscillators. The system of interest is defined by an harmonic potential dependent on q, the position operator of the system, with mass m, and *explicit Hamiltonian* vibrational frequency ω_{UO}. The oscillators in the single bath have masses $\{m_j\}$, frequencies $\{\omega_j\}$ and coupling constants $\{c_j\}$. The general, total, Hamiltonian is,

$$\mathrm{H_{tot}} = \mathrm{H_S} + \mathrm{H_B} + \mathrm{H_{SB}} + \mathrm{H_{SF}}, \tag{1}$$

where,

$$\mathrm{H_S} = |g\rangle\ \mathrm{h}_g\ \langle g| + |e\rangle\ \mathrm{h}_e\ \langle e|\,, \tag{2}$$

with

$$\mathrm{h}_g = \frac{\mathrm{p}^2}{2m} + \frac{1}{2}m\omega_{\mathrm{UO}}^2\mathrm{q}^2, \tag{3}$$

$$\mathrm{h}_e = \hbar\omega_{eg} + \frac{\mathrm{p}^2}{2m} + \frac{1}{2}m\omega_{\mathrm{UO}}^2(\mathrm{q}-d)^2, \tag{4}$$

$$\mathrm{H_B} = \sum_j \left[\frac{\mathrm{p}_j^2}{2m_j} + \frac{m_j\omega_j\mathrm{x}_j^2}{2}\right], \tag{5}$$

$$\mathrm{H_{SB}} = -\sum_j c_j\mathrm{x}_j\mathrm{q}, \tag{6}$$

and $\mathrm{p}, \mathrm{q}, \{\mathrm{p}_j\}, \{\mathrm{x}_j\}$ are the respective momentum and position operators for the system and the bath, and d is the displacement of the excited state potential energy surface.

In the context of this work, this system is extended to a two bath approach. This is achieved by canonically transforming the system frequency ω_{UO} into a separate spectral density. This is what becomes the undamped oscillator mode, and hence is why the system vibration is named UO in the one bath system Hamiltonian. Such a process transforms the molecular coordinate q into the electronic subsystem and the 'vibrational' subsystem (dependent on ω_{UO}) into the undamped (UO) bath coordinate, χ. Consequently, the system can be redefined from equation (1) with

$$\mathrm{H_S} = \left(\hbar\omega_{eg} - \frac{1}{2}m_{\mathrm{UO}}\omega_{\mathrm{UO}}^2 d^2\right)|e\rangle\langle e|\,, \tag{7}$$

and with a pair of bath contributions

$$\mathrm{H_B} = \mathrm{H_{UO}} + \mathrm{H_{LD}}, \tag{8}$$

$$\mathrm{H_{UO}} = \frac{\mathrm{p}^2}{2m_{\mathrm{UO}}} + \frac{1}{2}m_{\mathrm{UO}}\omega_{\mathrm{UO}}^2\chi^2, \tag{9}$$

and

$$\mathrm{H_{LD}} = \sum_j \left[\frac{\mathrm{p}_j^2}{2m_j} + \frac{m_j\omega_j\mathrm{x}_j^2}{2}\right], \tag{10}$$

which then couple to the system degrees of freedom via

$$\mathrm{H_{SB}} = \mathrm{H_{SUO}} + \mathrm{H_{SLD}}, \tag{11}$$

$$\mathrm{H_{SUO}} = -m_{\mathrm{UO}}\omega_{\mathrm{UO}}^2\,\chi\,d\ |e\rangle\langle e|\,, \tag{12}$$

$$= -S_{\mathrm{UO}}^{\mathrm{HR}}\,\chi\ |e\rangle\langle e|\,, \tag{13}$$

where the Huang-Rhys factor of the undamped mode is analogous to its associated 'Matsubara amplitude' from the spectral density $c_{\mathrm{UO}} = S_{\mathrm{UO}}^{\mathrm{HR}}$ and

$$\mathrm{H_{SLD}} = -\sum_j c_j\mathrm{x}_j\,|e\rangle\langle e|\,. \tag{14}$$

Once the bath contribution is split between two components, it is crucial to note that no explicit $\mathrm{H_{UOLD}} \propto \chi\,\mathrm{x}_j\ |e\rangle\langle e|$ component is included within $\mathrm{H_{SB}}$. In our model the excited state displacement, d, is defined implicitly from the reorganisation energy, λ_{UO}. Therefore this system has oscillators from the two baths with masses $\{m_j, m_{\mathrm{UO}}\}$, frequencies $\{\omega_j, \omega_{\mathrm{UO}}\}$, coupling constants $\{c_j, c_{\mathrm{UO}}\}$, and the respective momentum and position operators $\{\mathrm{p}_j, \mathrm{p}\}, \{\mathrm{x}_j, \chi\}$.

The system dynamics is initiated by a driving field, used to excite the fundamental transition, through

$$\mathrm{H_{SF}} = -\mu\cdot\left(\chi_{\mathrm{F}}E(t-\tau_p)\exp(-i\omega_{eg}t + i\mathbf{kr})\right) + \mathrm{c.c}, \tag{15}$$

where χ_{F} is the electronic field strength, ω_{eg} the fundamental frequency of the system's electronic transition, $\mathbf{k}$ is the associated wavevector, and $E(t-\tau_p)$ is the field envelope. The envelope is assumed to be Gaussian such that

$$E(t-\tau_p) = \exp\left(\frac{(t-\tau_p)^2}{2\varsigma^2}\right), \tag{16}$$

with a peak centre at τ_p and a variance, defined from the full-width-at-half-maximum (FWHM) as $2\varsigma\sqrt{2\ln(2)}$. Full details of the system field coupling can be found in Green et al. [31].

Given this description of the system and bath we can construct the density matrix, starting from the system in the vibronic basis. For a set of states $\{|\mathrm{q}_i, \mathrm{x}_i\rangle\}$ with corresponding transition probabilities $\{P_i\}$ the density matrix is equivalent to the outer product,

$$\rho(\mathrm{q},\mathrm{x}) = \sum_i P_i\,|\mathrm{q}_i,\mathrm{x}_i\rangle\langle\mathrm{q}_i,\mathrm{x}_i|\,. \tag{17}$$

To derive the equations of motion we use the path integral formalism. Introducing the time propagation operators we can find the density matrix at an arbitrary, non-zero time, t from an initial density matrix at time zero,

$$\rho_t(\mathrm{q},\mathrm{x}) = \exp\left(\frac{i\mathrm{H}(\mathrm{q},\mathrm{x})t}{\hbar}\right)\rho_0(\mathrm{q},\mathrm{x})\exp\left(\frac{-i\mathrm{H}(\mathrm{q},\mathrm{x})t}{\hbar}\right). \tag{18}$$

Next we apply the Born approximation so the system is initially in a factorisable state with respect to the thermally equilibrated bath,

$$\rho_0(\mathrm{q},\mathrm{x}) = \rho_{\mathrm{S}}(\mathrm{q})\rho_{\mathrm{B}}(\mathrm{x}), \tag{19}$$

which allows the reduced density matrix element to be expressed in path integral form, once the bath degrees of

freedom have been traced out[33,34]:

$$\rho(\mathrm{q}_t,\mathrm{q}_t',t)=\iint\int_{\mathrm{q}_0}^{\mathrm{q}_t}\int_{\mathrm{q}_0'}^{\mathrm{q}_t'}\exp\left(\frac{i\mathrm{S}_\mathrm{S}[\mathrm{q}_t]}{\hbar}\right)\times\exp\left(-\frac{i\mathrm{S}_\mathrm{S}[\mathrm{q}_t']}{\hbar}\right)\left(\prod_n\mathcal{F}_n[\mathrm{q}_t,\mathrm{q}_t']\right)\rho_\mathrm{S}(\mathrm{q}_0,\mathrm{q}_0',0)\times\mathcal{D}[\mathrm{q}_t]\mathcal{D}[\mathrm{q}_t']\ \mathrm{d}\mathrm{q}_0\ \mathrm{d}\mathrm{q}_0',\quad(20)$$

where $\int\mathcal{D}[\mathrm{q}_t]$ represents the functional integral. The action, denoted $\mathrm{S}_\mathrm{S}[\mathrm{q}_t;t]$, is associated with the corresponding system Hamiltonian, H_S.

The bath effects are contained within the Feynman and Vernon influence functional for the nth bath, and full details of the separation of system and bath degrees of freedom can be found within the original derivation [33,35,36]. Tanimura and Kubo[37] take a form of the influence functional which explicitly contains the fluctuation, $L_2^n(t)$,and dissipation, $iL_1^n(t)$[35], kernels of the system of interest and consequently the influence functional takes the form:

$$\mathcal{F}_n=\exp\left(-\frac{i}{\hbar}\int_0^t\int_0^\tau\mathrm{B}^\times(\mathrm{q}_t,\mathrm{q}_t';\tau)\times\left[iL_1^n(\tau-\tau')\mathrm{B}^\circ(\mathrm{q}_t,\mathrm{q}_t';\tau')+L_2^n(\tau-\tau')\mathrm{B}^\times(\mathrm{q}_t,\mathrm{q}_t';\tau')\right]\times\mathrm{d}\tau'\ \mathrm{d}\tau\right),\quad(21)$$

with the general form of the bath coupling operator B in the vibronic basis obeying, $\mathrm{B}^\times(\tau)=\mathrm{B}^\times(\mathrm{q}_t;\tau)-\mathrm{B}^\times(\mathrm{q}_t';\tau)$, and $\mathrm{B}^\circ(\tau)=\mathrm{B}^\times(\mathrm{q}_t;\tau)+\mathrm{B}^\times(\mathrm{q}_t';\tau)$, respectively. This form is used within one bath models where there is an explicit q, system, coordinate within the Hamiltonian and a system vibration. After canonical transformation from a vibronic system basis to an electronic system basis the continuous nuclear paths in system space, $q(\tau)$, become discrete system states $s(\tau)$ as a consequence of the removal of system vibrations. This leads to the simplification of the influence functional to

$$\mathcal{F}_n=\exp\left(-\frac{i}{\hbar}\int_0^t\int_0^\tau\mathrm{B}^\times(\mathrm{s}_t,\mathrm{s}_t';\tau)\times\left[iL_1^n(\tau-\tau')\mathrm{B}^\circ(\mathrm{s}_t,\mathrm{s}_t';\tau')+L_2^n(\tau-\tau')\mathrm{B}^\times(\mathrm{s}_t,\mathrm{s}_t';\tau')\right]\times\mathrm{d}\tau'\ \mathrm{d}\tau\right),\quad(22)$$

where the bath coupling operator B obeys the commutation and anti-commutation relations of the electronic system state, respectively, $\mathrm{B}^\times(\tau)=s(\tau)-s'(\tau)$, and $\mathrm{B}^\circ(\tau)=s(\tau)+s'(\tau)$. Such a change is necessary when moving to a two bath model. The explicit form of the bath coupling operator used in this work is

$$\mathrm{B}=\mathrm{B}_1+\mathrm{B}_2,\quad(23)$$

$$=\Big(|e\rangle\langle e|+(|e\rangle\langle g|+|g\rangle\langle e|)\Big)\otimes\mathrm{I}_\mathrm{vib}.\quad(24)$$

The kernels can be expressed by the spectral distribution as

$$L_2^n(t)=\int_0^\infty J_n(\omega)\cos(\omega t)\coth\left(\frac{\beta\hbar\omega}{2}\right)\mathrm{d}\omega,\quad(25)$$

$$iL_1^n(t)=-\int_0^\infty J_n(\omega)\sin(\omega t)\ \mathrm{d}\omega.\quad(26)$$

We split the environment into two major contributions: an overdamped bath (denoted LD for Lorentz-Drude), which is appropriate for Gaussian noise and an undamped oscillator (UO) mode. The approach is similar to our BVM, where the undamped oscillator mode is subsumed canonically into the spectral density. This results in a form of the BVM, but in the limit of a zero linewidth vibration, where the canonical damping is zero. The spectral density can be written,

$$J(\omega)=J_\mathrm{LD}(\omega)+J_\mathrm{UO}(\omega),\quad(27)$$

where

$$J_\mathrm{LD}(\omega)=\frac{2\eta_\mathrm{LD}\gamma_\mathrm{LD}\omega_0^2\omega}{(\omega_0-\omega)^2+(\gamma_\mathrm{LD}\omega)^2},$$

which can be further simplified to the Lorentz-Drude form given that $\gamma_\mathrm{LD}\gg\omega_0$ such that $\Lambda_\mathrm{LD}=\omega_0^2/\gamma_\mathrm{LD}$,

$$J_\mathrm{LD}(\omega)=\frac{2\eta_\mathrm{LD}\omega\Lambda_\mathrm{LD}}{\omega^2+\Lambda_\mathrm{LD}^2},\quad(28)$$

and

$$J_\mathrm{UO}=\frac{1}{2}S_\mathrm{UO}^\mathrm{HR}\omega\left(\delta(\omega-\omega_\mathrm{UO})+\delta(\omega+\omega_\mathrm{UO})\right),\quad(29)$$

with $S_\mathrm{UO}^\mathrm{HR}=\lambda_\mathrm{UO}/\omega_\mathrm{UO}$. This form of the undamped part of spectral density matches that which is used in Seibt et al.[38,39], with the exception of the factor, ω_UO. This ensures that the spectral density has an amplitude proportional to the reorganisation energy, λ_UO. We note that this is equivalent to applying a single delta function of the form $J(\omega)=S_\mathrm{UO}^\mathrm{HR}\omega_\mathrm{UO}\delta(\omega-\omega_\mathrm{UO})$. The next step is to decompose the respective bath contributions, according to the Matsubara scheme, in order to explicitly incorporate time-dependent, but temperature-independent, Matsubara decomposition coefficients and frequencies[38,39] into the correlation function. We perform this process for each component of the total spectral density piecewise. Starting with the Lorentz-Drude component we decompose the correlation function using complex contour integration[18], resulting in:

$$L_\mathrm{LD}(t)=\eta_\mathrm{LD}\Lambda_\mathrm{LD}\left(\cot\left(\frac{\beta\hbar\Lambda_\mathrm{LD}}{2}\right)-i\right)e^{-\Lambda_\mathrm{LD}t}+\sum_{n=1}^\infty\frac{2\eta_\mathrm{LD}\Lambda_\mathrm{LD}\nu_n}{\beta\hbar(\nu_n^2-\Lambda_\mathrm{LD}^2)}e^{-\nu_n t},\quad(30)$$

which can be simplified by denoting,

$$d_0 = \eta_{\rm LD}\Lambda_{\rm LD}\left(\cot\left(\frac{\beta\hbar\Lambda_{\rm LD}}{2}\right) - i\right), \quad \nu_0 = \Lambda_{\rm LD}, \quad (31)$$

$$d_n = \frac{2\eta_{\rm LD}\Lambda_{\rm LD}}{\beta\hbar}\left(\frac{\nu_n}{\nu_n^2 - \Lambda_{\rm LD}^2}\right), \quad \nu_n = \frac{2n\pi}{\beta\hbar}, \quad (32)$$

such that

$$L_{\rm LD}(t) = \sum_{n=0}^{\infty} d_n e^{-\nu_n t}. \quad (33)$$

Next we decompose the undamped oscillator mode component, proposed in reference 17, through the sifting property of the delta function resulting in:

$$L_{\rm UO}(t) = \frac{S_{\rm UO}^{\rm HR}\omega_{\rm UO}}{2}\Bigg[\exp(-i\omega_{\rm UO}t)\left(\coth\left(\frac{\beta\hbar\omega_{\rm UO}}{2}\right)+1\right) + \exp(i\omega_{\rm UO}t)\left(\coth\left(\frac{\beta\hbar\omega_{\rm UO}}{2}\right) - 1\right)\Bigg]. \quad (34)$$

From this we have generated the Matsubara decomposition coefficients and frequencies for the second bath:

$$c_1 = c_2^* = \frac{1}{2}S_{\rm UO}^{\rm HR}\omega_{\rm UO}\left(\coth\left(\frac{\beta\hbar\ \omega_{\rm UO}}{2}\right) + 1\right), \quad (35)$$

$$c_2 = c_1^* = \frac{1}{2}S_{\rm UO}^{\rm HR}\omega_{\rm UO}\left(\coth\left(\frac{\beta\hbar\ \omega_{\rm UO}}{2}\right) - 1\right), \quad (36)$$

$$\gamma_1 = \gamma_2^* = i\omega_{\rm UO}, \quad (37)$$

$$\gamma_2 = \gamma_1^* = -i\omega_{\rm UO}. \quad (38)$$

Additionally, the coordinates are moved into a coherent state basis transforming $\mathrm{a}_i^\dagger$ and a_i, to x_j and p_j for the environment modes $\{j\}$. This representation uses

$$|\phi\rangle = \exp\left(\sum_i \phi_i \mathrm{a}^\dagger\right)|0\rangle, \quad (39)$$

where $|0\rangle$ is the system vacuum sate, ϕ_i are complex numbers, and ϕ_i^* their complex conjugates such that

$$\mathrm{a}_i|\phi\rangle = \phi_i|\phi\rangle, \quad (40)$$

$$\langle\phi|\mathrm{a}_i^\dagger = \langle\phi|\phi_i^*. \quad (41)$$

This is a movement from trajectories in physical space to trajectories of coherent states: s, x, s′ and x′ to $\mathrm{Q}_t = (\phi^*(\tau), \phi(\tau))$ and $\mathrm{Q}_t' = (\phi'^*(\tau), \phi'(\tau))$. Given these decompositions, and in a manner equivalent to the process in Ishizaki Tanimura[40], we construct the total influence function as:

$$\mathcal{F} = \prod_n^t \mathcal{F}_n = \mathcal{F}_{\rm LD} \times \mathcal{F}_{\rm UO}, \quad (42)$$

$$\mathcal{F}_{\rm UO} = \exp\Bigg(-\frac{1}{\hbar}\int_0^t\int_0^\tau \sum_k \mathrm{B}_k^\times(\mathrm{Q}_t, \mathrm{Q}_t'; \tau)\times \exp(-\gamma_k(\tau-\tau'))\Theta_k(\mathrm{Q}_t, \mathrm{Q}_t'; \tau')\ \mathrm{d}\tau'\ \mathrm{d}\tau\Bigg). \quad (43)$$

where,

$$\Theta_k = \frac{1}{2}\Bigg[(c_k - c_k^*)\mathrm{B}_k^\circ(\mathrm{Q}_t, \mathrm{Q}_t'; \tau') + (c_k + c_k^*)\mathrm{B}_k^\times(\mathrm{Q}_t, \mathrm{Q}_t'; \tau')\Bigg], \quad (44)$$

and

$$\mathcal{F}_{\rm LD} = \exp\Bigg(-\frac{1}{\hbar}\int_0^t\int_0^\tau \mathrm{B}^\times(\mathrm{Q}_t, \mathrm{Q}_t'; \tau)\vartheta(\mathrm{Q}_t, \mathrm{Q}_t'; \tau')\Lambda_{\rm LD} \times \exp(-\Lambda_{\rm LD}(\tau-\tau'))\ \mathrm{d}\tau'\ \mathrm{d}\tau\Bigg) \times \prod_{n=1}^{\infty}\exp\Bigg(-\frac{1}{\hbar}\int_0^t\int_0^\tau \mathrm{B}^\times(\mathrm{Q}_t, \mathrm{Q}_t'; \tau)\Psi_n(\mathrm{Q}_t, \mathrm{Q}_t'; \tau')\nu_n\exp(-\nu_n(\tau-\tau'))\ \mathrm{d}\tau'\ \mathrm{d}\tau\Bigg). \quad (45)$$

where,

$$\vartheta = \eta_{\rm LD}\Bigg[\cot\left(\frac{\beta\hbar\Lambda_{\rm LD}}{2}\right)\mathrm{B}^\times(\mathrm{Q}_t, \mathrm{Q}_t'; \tau') - i\mathrm{B}^\circ(\mathrm{Q}_t, \mathrm{Q}_t'; \tau')\Bigg], \quad (46)$$

$$\Psi_n = \sum_{n=1}^{\infty}\frac{2\eta_{\rm LD}\Lambda_{\rm LD}\nu_n}{\beta\hbar(\nu_n^2 - \Lambda_{\rm LD}^2)}\mathrm{B}^\times(\mathrm{Q}_t, \mathrm{Q}_t'; \tau'). \quad (47)$$

For a value of K, which satisfies $\nu_K = 2\pi K/\beta\hbar \gg \omega_0$, where ω_0 is the fundamental frequency of the system, then $\nu_n\exp(-\nu_n(\tau-\tau')) \approx \delta(\tau-\tau')$ for $n \geq K+1$. This simplifies the influence functional, equation (48).

We introduce the auxiliary operator, $\rho_{j_1\ldots j_K}^{(m,l_k)}$, by its matrix element, in equation (49), as[40]

$$\mathcal{F} \approx \exp\left(-\int_0^t \int_0^\tau \sum_k \mathrm{B}_k^\times(\mathrm{Q}_t, \mathrm{Q}'_t; \tau) \exp(-\gamma_k(\tau - \tau'))\Theta_k(\mathrm{Q}_t, \mathrm{Q}'_t; \tau') \, \mathrm{d}\tau' \, \mathrm{d}\tau \right) \times$$
$$\exp\left(-\int_0^t \mathrm{B}^\times(\mathrm{Q}_t, \mathrm{Q}'_t; \tau) \exp(-\Lambda_{\mathrm{LD}}\tau) \left[-\int_0^\tau \Lambda_{\mathrm{LD}} \vartheta(\mathrm{Q}_t, \mathrm{Q}'_t; \tau') \exp(\Lambda_{\mathrm{LD}}\tau') \, \mathrm{d}\tau' \right] \mathrm{d}\tau \right) \times$$
$$\prod_{n=1}^{K} \exp\left(-\int_0^t \mathrm{B}^\times(\mathrm{Q}_t, \mathrm{Q}'_t; \tau) \exp(-\nu_n\tau) \left[-\int_0^\tau \nu_n \Psi_n(\mathrm{Q}_t, \mathrm{Q}'_t; \tau') \exp(\nu_n\tau') \, \mathrm{d}\tau' \right] \mathrm{d}\tau \right) \times$$
$$\prod_{n=K+1}^{\infty} \exp\left(\int_0^t \mathrm{B}^\times(\mathrm{Q}_t, \mathrm{Q}'_t; \tau) \Psi_n(\mathrm{Q}_t, \mathrm{Q}'_t; \tau) \, \mathrm{d}\tau \right). \quad (48)$$

$$\rho^{(m,l_k)}_{j_1 \ldots j_K}(\mathrm{Q}_t, \mathrm{Q}'_t; t) = \int_{\mathrm{Q}_t(t_0)}^{\mathrm{Q}_t(t)} \int_{\mathrm{Q}'_t(t_0)}^{\mathrm{Q}'_t(t)} \exp\left(\frac{iS_{\mathrm{S}}[\mathrm{Q}_t, \mathrm{Q}'_t]}{\hbar} \right) \mathcal{F} \exp\left(\frac{-iS_{\mathrm{S}}[\mathrm{Q}_t, \mathrm{Q}'_t]}{\hbar} \right) \rho(\mathrm{Q}_{t_0}, \mathrm{Q}'_{t_0}; t_0) \times$$
$$\prod_k \left\{ \int_0^t \exp(-\gamma_k(t - \tau'))\Theta_k(\mathrm{Q}_t, \mathrm{Q}'_t; \tau') \, \mathrm{d}\tau' \right\}^{l_k} \left\{ \exp(-\Lambda_{\mathrm{LD}}t) \left[-\int_0^t \Lambda_{\mathrm{LD}} \vartheta(\mathrm{Q}_t, \mathrm{Q}'_t; \tau') \exp(\Lambda_{\mathrm{LD}}\tau') \, \mathrm{d}\tau' \right] \right\}^m \times$$
$$\prod_{n=1}^{K} \left\{ \exp(-\nu_n t) \left[-\int_0^t \nu_n \Psi_n(\mathrm{Q}_t, \mathrm{Q}'_t; \tau') \exp(\nu_n\tau') \, \mathrm{d}\tau' \right] \right\}^{j_n} \mathcal{D}[\mathrm{Q}_t] \, \mathcal{D}[\mathrm{Q}'_t]. \quad (49)$$

for non-negative integers $l_k, m, j_1, \ldots, j_K$. Differentiating equation (49) with respect to time, and then computing the path integrals, results in the following equations of motion[18]:

$$\frac{\partial}{\partial t}\rho^{(m,l_k)}_{j_1 \ldots j_K} = \left(-\frac{i}{\hbar}\mathrm{H}_{\mathrm{S}}^\times - \sum_k (l_k\gamma_k + m\Lambda_{\mathrm{LD}}) - \sum_{n=1}^{K} j_n\nu_n + \sum_{n=K+1}^{\infty} \mathrm{B}_k^\times \Psi_n \right) \rho^{(m,l_k)}_{j_1 \ldots j_K} -$$
$$\sum_k l_k \Theta_k \rho^{(m,l_k-1)}_{j_1 \ldots j_K} - m\Lambda_{\mathrm{LD}} \vartheta \rho^{(m-1,l_k)}_{j_1 \ldots j_K} - \sum_{n=1}^{K} j_n \nu_n \Psi_n \rho^{(m,l_k)}_{j_1 \ldots j_{n-1} \ldots j_K} -$$
$$\left(\mathrm{B}^\times \rho^{(m+1,l_k)}_{j_1 \ldots j_K} + \sum_k \mathrm{B}_k^\times \rho^{(m,l_k+1)}_{j_1 \ldots j_K} \right) - \sum_{n=1}^{K} \mathrm{B}^\times \rho^{(m,l_k)}_{j_1 \ldots j_{n+1} \ldots j_K}. \quad (50)$$

Upon first inspection it may appear that there is an absent factor of γ_k in the creation term from the $(l_k - 1)$th Matsubara axis, however this is not the case. Based on the reduction criteria for the infinite Matsubara components, which for the overdamped contribution is:

$$\nu_K = \frac{2\pi K}{\beta\hbar} \gg \omega_0, \quad (51)$$

we reduce to a delta function for a sufficient value of K. However, such a reduction cannot be performed for the undamped component. The undamped contribution introduces a pair of Matsubara decomposition coefficients and frequencies, as opposed to an infinite number, and as such a sufficient value of K being chosen is unlikely. This lack of reduction motivates the current derivation and it results in factors of $(c_k \pm c_k^*)$ in Θ_k, which (based on the form of c_k in equation (35)) accounts for the apparent missing factor of γ_k.

The condition,

$$\sum_k (l_k\gamma_k + m\Lambda_{\mathrm{LD}}) + \sum_{n=1}^{K} j_n\nu_n \gg \frac{\omega_0}{\min(\mathcal{I}(\nu_k), \mathcal{R}(\nu_n))}, \quad (52)$$

$$\implies \quad \Gamma_{\max} = 10 \, \max\Big(\mathcal{I}(\gamma_k)\Big). \quad (53)$$

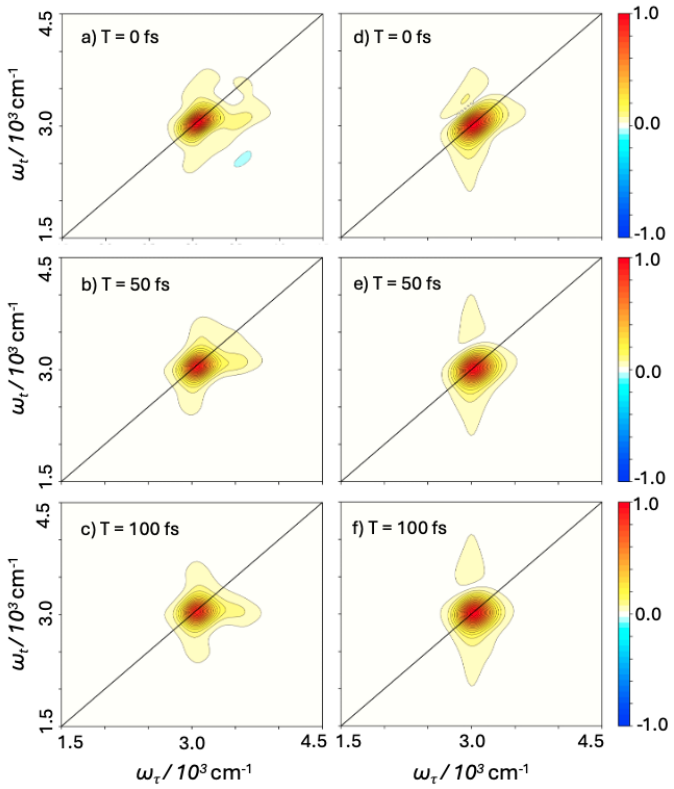

FIG. 2: Two-dimensional electronic spectra (2DES) for the BVM system, column 1, and the LDUO-HEOM, column 2. Each column presents spectra for three population times, $T = 0$, 50, and 100 fs.

terminates the over- *and* undamped axes. This leads to hierarchy volumes that are similar for both baths.

Subsequently, the infinite hierarchy can be truncated by the terminator[31,41]:

$$\frac{\partial}{\partial t}\rho^{(m,l_k)}_{j_1\ldots j_K} \approx \left(-\frac{i}{\hbar}\mathrm{H}^{\times}_{\mathrm{S}} - \sum_k l_k\gamma_k + \sum_{n=K+1}^{\infty} \mathrm{B}^{\times}\Psi_n\right)\rho^{(m,l_k)}_{j_1\ldots j_K}. \tag{54}$$

Here, the phonon contributions from the system characteristic damping rate vanish as they are a purely real decay, whereas the purely imaginary oscillating components persist. This can be rationalised through the limit of infinite time, all contributions with an associated damping will vanish leaving only oscillatory components after the application of the Markovian criterion. This can be rewritten as[42]

$$\frac{\partial}{\partial t}\rho^{(m,l_k)}_{j_1\ldots j_K} \approx \left(-\frac{i}{\hbar}\mathrm{H}^{\times}_{\mathrm{S}} - i(l_0 - l_1)\omega_{\mathrm{UO}} + \sum_{n=K+1}^{\infty} \mathrm{B}^{\times}\Psi_n\right)\rho^{(m,l_k)}_{j_1\ldots j_K}. \tag{55}$$

Since the undamped oscillator component contributes a pair of Matsubara decomposition frequencies and coefficients, we expect the number of hierarchy elements to be only slightly greater than that of an overdamped HEOM.

IV. NUMERICAL SIMULATIONS

The objective of the above derivation is to produce a version of HEOM that will give accurate spectra for systems in which an undamped oscillation is coupled to an overdamped spectral density. This new model is designed to eliminate the additional damping that occurs from an underdamped spectral density with finite linewidth. We apply the LDUO-HEOM to nonlinear optical spectroscopy to test the effect of superfluous damping on quality of 2D spectra. Note that in generating the spectra, instead of using the squared macroscopic polarisation, in the case of an undamped mode it is necessary to sum the absorptive component with the π^{c} phase flipped dispersive component in order to preserve the spectral broadening.

To benchmark the new HEOM, a two-level system with a fundamental transition frequency of $\omega_{eg} = 3000$ cm^{-1} is used. This is coupled to a harmonic oscillator mode of frequency $\omega_0 = 500$ cm^{-1}, and excited by a laser field, resonant with the electronic transition, at a field strength of $\chi_{\mathrm{F}} = 10^3\,\mathrm{V\,m^{-1}}$, coupled via $\mu = \sigma_x$. Full details of the model can be found in Green et al. [31]

The bath parameters, used in these simulations are $\eta = (50, 50)$ cm^{-1}, and $\gamma = (100, 2500)$ cm^{-1}, for the BVM, the first value in parentheses corresponds to the overdamped environment and the second the canonically

subsumed mode resulting in an underdamped bath, and $\eta = 50$ cm^{-1}, $\Lambda = 100$ cm^{-1}, and $\lambda_{\mathrm{UO}} = 0.5$ cm^{-1}, for the LDUO-HEOM.

The left column of figure 2 shows the BVM case while the right shows the LDUO-HEOM case for the identical system. The two sets of spectra in figure 2 are qualitatively similar, both in terms of peak positions and broadening, demonstrating that the LDUO-HEOM is effective in modelling the BVM in the limit of vanishing canonical damping. Both the BVM and LDUO-HEOM spectra present an inhomogeneously broadened fundamental peak which becomes more rounded for later population times, indicating spectral diffusion at later times. A notable consequence of the undamped mode is a vertical stretching (along the emission axis) of the peaks. This is expected and occurs because of the longer-lived oscillation of the polarisation that results from the undamped contribution to the total spectral density.

One of the most major benefits of this new approach, apart from the removal of the artificial damping, is the reduction in computational cost. In order to generate these spectra there is an equilibration step, an evolution, and calculation of 2D spectra. In the case of the BVM these steps take 1 hour 29 mins, 3 hours 34 mins, and 16 hours and 19 mins, respectively. However, in the LDUO-HEOM the same steps took ~ 30 seconds, ~ 1 minute, and ~ 3 minutes, respectively, on the same cluster. This means that the LDUO-HEOM took 0.56% of the time the BVM did, or better, and represents an improvement of at least 99.4%.

V. ANALYSIS OF BATH COMMUNICATION

Having shown that the two-bath LDUO-HEOM approach produces 2DES which are in qualitative agreement with analogous single-bath models, we now consider communication (i.e. information transfer) between the two baths. Firstly we note that fully coupled, product spectral densities and full generating functional approaches are yet to be applied to any two-bath models. When the baths are not directly coupled, the degree of implicit communication between the two constituent baths is dictated solely by their couplings to the quantum system. A previous study, Seibt et al. proposed models in which sub-components of the total system are explicitly coupled together via Herzberg-Teller coupling through generating function approaches.[38] In our model, the system-bath boundary is not as clear cut because hybridisation between the degrees of freedom of the environment and the molecule is implicit in the construction of the LDUO-HEOM. While the appearance of a vibronic progression in the 2DES, above, indicates that the electronic degrees of freedom from the system couple with vibrational information contained in the spectral density, this does not confirm whether the individual baths interact with each other in the absence of explicit bath-bath coupling. To quantify any explicit correlations between the baths, which would imply information transfer between them, we apply the bath coordinate expectation value approach proposed by Zhu et al[43,44]. The system-bath interaction term is taken as

$$\mathrm{H_{SB}} = -\sum_j c_j \mathrm{x}_j \mathrm{B} \equiv -\mathrm{F} \otimes \mathrm{B}, \tag{56}$$

where $\mathrm{F} = \sum_j c_j \mathrm{x}_j$ is a collective bath coordinate for the system. Zhu et al. showed that the expectation values of the collective bath coordinate, F, can be tracked directly from the density matrix and its associated ADOs. The structure of the bath coordinate is such that it defines environmental polarisation effects in fermionic systems and energetic fluctuations due to excitation of the environment. In both instances, this quantifies the degree of the system-bath interaction. In HEOM methodologies the information exchanged between a system and bath is distributed throughout the ADOs and as such, the ADOs are intrinsic to the calculation of expectation operators of the bath coordinate. The hierarchy structure reflects the properties of the OQS including the bath relaxation rate and system-bath coupling strength.

Each Matsubara frequency corresponds to an independent axis within the hierarchy, and ADOs along this dimension contain quantum information in terms of integer multiples of the Matsubara frequency[18]. There have been a number of different ways to represent the ADO hierarchy geometrically presented over the years.[24,32,40,43–45] In our analysis, we have found that a pyramidal structure is very intuitive for representing the flow of information through the ADOs, from the density operator in the apex. Figure 3 shows a simple example of a hierarchical structure with three Matsubara dimensions ν_k, $k \in \{1, 2, 3\}$. Tiers are defined as ADOs with a common sum of indices. For example, all Matsubara vectors with a total index sum of 1 are first tier, and are shown on the blue surface within the hierarchy volume in fig. 3. Each tier exists as a surface within the Matsubara space which corresponds to a physical cutoff speed at which phonon modes are considered to be Markovian. Physically this corresponds to the extent to which information is able to extend through the hierarchy. At Γ_{max}, or greater, ADOs contain phonon states which are faster than the non-Markovian cutoff and as such these ADOs will be outside the hierarchy volume in which information can return to the density matrix.

Given the definition of tiers within the hierarchy, we calculate the bath coordinate expectation values at each tier in the hierarchy. To simplify the indexing, we define three vectors; a collective Matsubara frequency index, a coefficient index, and Matsubara index for the total HEOM as

$$\nu_\alpha^{\mathrm{LDUO}} = [\gamma_k,\, \Lambda_{\mathrm{LD}},\, \nu_n], \tag{57}$$

$$e_\alpha = [c_k,\, d_0,\, d_n], \tag{58}$$

$$n_\alpha = [l_k,\, m,\, j_n]. \tag{59}$$

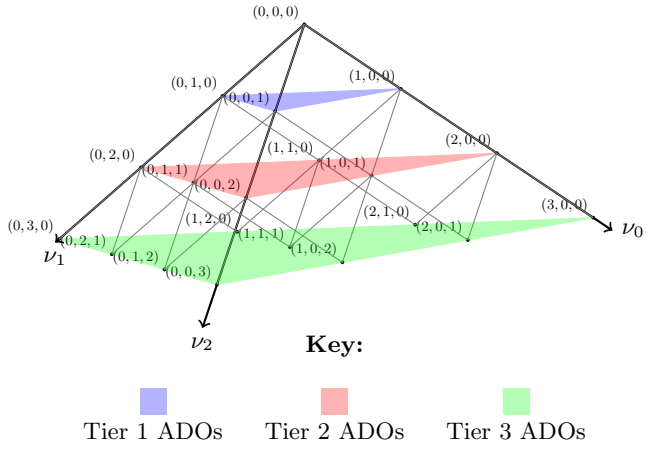

FIG. 3: A generalised, arbitrary hierarchy diagram showing the ADO Matsubara vectors for a system with three Matsubara dimensions, ν_k, $k = \{1, 2, 3\}$. Tiers are shown as coloured surfaces within the closed pyramidal volume. This schematic is for visualisation and typical, real, hierarchies can contain many more dimensions than three.

This means that the ADOs can be rewritten as:

$$\rho^{(m,l_k)}_{j_1\ldots j_K} \equiv \rho_{n_\alpha}, \tag{60}$$

with the associated correlation function

$$L_{\rm tot}(t) = \sum_\alpha e_\alpha e^{-\nu_\alpha^{\rm LDUO} t}. \tag{61}$$

Expectation values of the coordinate F can be generated through probing the Hamiltonian with a classical field, $f(t)$,[43,46]

$$\mathrm{H}_{\rm tot} \to \mathrm{H}_f = \mathrm{H}_{\rm S} + \mathrm{H}_{\rm B} + \mathrm{H}_{\rm SB} + \mathrm{H}_{\rm SF} - f(t)\,\mathrm{F}. \tag{62}$$

In the interaction picture this means we can define $\rho_f(t) = \mathrm{U}_f\,\rho(0)\mathrm{U}_f^\dagger$ as the total evolved state using H_f with $\mathrm{U}_f(t) = \mathcal{T}\exp\left(i\int_0^t f(\tau)\mathrm{F}(\tau)\,\mathrm{d}\tau\right)$, where $\mathcal{T}$ is the time-ordering operator. Then by taking n variational derivatives with respect to f it is possible to generate nth order moments of the coordinate F:[43,46]

$$\frac{\delta}{\delta f(t_1)}\left(\mathrm{Tr}_{\rm B}\Big(\rho_f(t)\Big)\right)\Big|_{f=0} = i\Theta(t-t_1)\mathrm{Tr}_{\rm B}\Big(\mathrm{F}(t_1)\rho_f(t)\Big), \tag{63}$$

$$\begin{aligned}\frac{\delta^2}{\delta f(t_2)\delta f(t_1)}\left(\mathrm{Tr}_{\rm B}\Big(\rho_f(t)\Big)\right)\Big|_{f=0} = \\ -\Theta(t-t_2)\Theta(t_2-t_1)\mathrm{Tr}_{\rm B}\Big(\mathrm{F}(t_2)\mathrm{F}(t_1)\rho_f(t)\Big) - \\ \Theta(t-t_1)\Theta(t_1-t_2)\mathrm{Tr}_{\rm B}\Big(\mathrm{F}(t_1)\mathrm{F}(t_2)\rho_f(t)\Big),\end{aligned} \tag{64}$$

$$\begin{aligned}\frac{\delta^n}{\delta f(t_n)\ldots f(t_1)}\left(\mathrm{Tr}_{\rm B}\Big(\rho_f(t)\Big)\right)\Big|_{f=0} = \\ i^n\Theta(t-t_n)\ldots\Theta(t_2-t_1)\mathrm{Tr}_{\rm B}\Big(\mathrm{F}(t_n)\ldots\mathrm{F}(t_1)\rho_f(t)\Big) + \\ (\text{time perturbations}),\end{aligned} \tag{65}$$

where Θ is the Heaviside function. For Gaussian baths this can be reduced, using the Wick/Isserlis formula,[47,48] to sums of products of pairs of two-point correlators ($L_{\rm tot}(t)$). Upon integration by parts the Heaviside functions yield static-time boundary conditions, $L_{\rm tot}(0)$ which are resolved through application of Kubo's symmetric condition $\Theta(0) = \frac{1}{2}$.[49] Consequently, the simultaneous time component can be written as

$$L_{\rm tot}(0) \equiv A_0 = \lim_{t\to 0}\frac{L_{\rm tot}(t) + L_{\rm tot}(-t)}{2}, \tag{66}$$

$$= \int_0^\infty \frac{J_{\rm tot}(\omega)}{\pi}\coth\Big(\tfrac{\beta\hbar\omega}{2}\Big)\,\mathrm{d}\omega, \tag{67}$$

$$= \sum_\alpha \mathcal{R}(e_\alpha). \tag{68}$$

This process yields expectation values (for $n = \{1, 2\}$) of F as

$$\mathrm{F}^{(n)} = \mathrm{Tr}_{\rm B}\Big(\mathrm{F}^n\rho_{\rm tot}\Big), \tag{69}$$

or

$$\mathrm{F}^{(1)}(t) = -\sum_{\text{tier 1}}\rho_{n_\alpha}(t), \tag{70}$$

$$\mathrm{F}^{(2)}(t) = A_0\rho_{\rm S}(t) - \underbrace{\sum_{\text{tier 2}}\rho_{n_\alpha}(t)}_{n_\alpha = 0,\text{ or } 2} - 2\underbrace{\sum_{\text{tier 2}}\rho_{n_\alpha}(t)}_{n_\alpha = 0,\text{ or } 1}, \tag{71}$$

where quantities with bracketed powers are expectation values of the stated order, and are matrix valued. From these formulae it is clear that static time contributions, A_0 are $\in \mathbb{R}_+$ for Hermitian bath coordinates F, however, ADOs within the hierarchy are defined as $\rho_{n_\alpha} \in \mathbb{C}^{d\times d}$, dim: d. As a result of this $\mathrm{F}^{(n)} \in \mathbb{C}$ where real valued components relate to the fluctuation dynamics, and imaginary portions to the dissipation, equivalent to contributions from the fluctuation dissipation integral

$$L_{\rm tot}(t) = \int_0^\infty J_{\rm tot}(\omega)\left(\coth(\tfrac{\beta\hbar\omega}{2})\cos(\omega t) - i\sin(\omega t)\right)\mathrm{d}\omega. \tag{72}$$

For this reason we define symmetric and anti-symmetric, real valued, expectation values for the fluctuation and dissipation, X and Y, respectively. We note that an analogous, imaginary, static time quantity at $t = 0$ is the Lamb-shift term which is usually contained within a Hamiltonian renormalisation and not a correlation function. Given

$$\mathcal{H}[Z] = \frac{Z + Z^\dagger}{2}, \quad \text{and} \quad \mathcal{A}[Z] = \frac{Z - Z^\dagger}{2i}, \tag{73}$$

$$\mathrm{X}^{(1)} = -\sum_{\text{tier 1}} \mathcal{H}[\rho_{n_\alpha}], \quad \sum_\alpha n_\alpha = 1, \tag{74}$$

$$\mathrm{X}^{(2)} = \underbrace{\mathcal{R}(\mathrm{A}_0)\rho_0}_{=A_0\rho_0} + \underbrace{\sum_{\text{tier 2}} \mathcal{H}[\rho_{n_\alpha}]}_{n_\alpha=0,\text{ or }2} + 2\underbrace{\sum_{\text{tier 2}} \mathcal{H}[\rho_{n_\alpha}]}_{n_\alpha=0,\text{ or }1}, \quad \sum_\alpha n_\alpha = 2, \tag{75}$$

and

$$\mathrm{Y}^{(1)} = -\sum_{\text{tier 1}} \mathcal{A}[\rho_{n_\alpha}], \quad \sum_\alpha n_\alpha = 1, \tag{76}$$

$$\mathrm{Y}^{(2)} = \underbrace{\mathcal{I}(\mathrm{A}_0)\rho_0}_{=0} + \underbrace{\sum_{\text{tier 2}} \mathcal{A}[\rho_{n_\alpha}]}_{n_\alpha=0,\text{ or }2} + 2\underbrace{\sum_{\text{tier 2}} \mathcal{A}[\rho_{n_\alpha}]}_{n_\alpha=0,\text{ or }1}, \quad \sum_\alpha n_\alpha = 2. \tag{77}$$

Higher orders of the bath coordinate expectation values can be generated from the recursion relation:

$$\mathrm{X}^{(n+1)} = \sum_{i=0}^{n+1} L_i^{(n+1)} \sum_{\text{tier } i} \frac{i\,!}{\prod_\alpha n_\alpha\,!} \mathcal{H}[\rho_{n_\alpha}], \quad \sum_\alpha n_\alpha = i, \tag{78}$$

$$L_i^{(n+1)} = -L_{i-1}^{(n)} + nA_0 L_i^{(n-1)}, \tag{79}$$

and

$$\mathrm{Y}^{(n+1)} = \sum_{i=0}^{n+1} M_i^{(n+1)} \sum_{\text{tier } i} \frac{i\,!}{\prod_\alpha n_\alpha\,!} \mathcal{A}[\rho_{n_\alpha}], \quad \sum_\alpha n_\alpha = i, \tag{80}$$

$$M_i^{(n+1)} = -M_{i-1}^{(n)}, \tag{81}$$

with $L_0^0 = M_0^0 = 1$. In this work we are primarily interested in the first two orders of the bath coordinate expectation value because the focus is on comparing one- and two-component spectral densities. The interested reader should refer to Zhu et al.[43,44] for further details on higher orders of the fluctuation expectation values.

In order to facilitate a direct comparison of the constituent modes we consider projections of the collective bath coordinate for each of the modes in turn. Geometrically, this corresponds to taking the sealed hierarchy volume from fig. 3 and projecting it to a closed surface. In this way we are able to generate bath coordinate expectation values for the independent LD and UO components, as well as for the full LDUO. Figure 4 demonstrates the process of projecting out components of the collective bath coordinate so that only ADOs associated with the left face of the pyramid are extracted.

Figure 5 presents a decomposition of the bath coordinate expectation values $\mathrm{X}^{(1)}(t)$ and $\mathrm{Y}^{(1)}(t)$ for the LDUO model and its isolated constituents: a pure undamped oscillator (UO), a pure overdamped Lorentz–Drude bath (LD), and a canonical two-bath model (LDUO). These results are treated as first order moments which present the mean coordinate of the bath.

In the top left panel, the projected undamped component of the LDUO model is shown. Here we see an oscillatory structure with the amplitude of the expectation values gradually shrinking over the lifetime of the trajectory consistent with a mean bath coordinate reaching equilibrium. The oscillations arise from the coherent accumulation of energy via the system from the indirect bath-system-bath coupling in the LDUO model. The undamped mode lacks a dissipation channel and hence progress towards equilibrium is hindered, in this projected subspace, and the bath continues to build up displacement as it mirrors the system's dynamics. We further note that, while equilibrium might not be reached with a subspace of the Matsubara volume, equilibrium would eventually be reached by the total system overall. The top right panel shows the isolated UO response which is further decomposed into the contributions from its two constituent Matsubara coefficients, c_k from equation (35), (each associated with the Matsubara frequencies $\pm i\omega_{\mathrm{UO}}$) in Figure 6 , that is, a trajectory with a single undamped bath. The bath dynamics are governed by a pair of purely imaginary frequencies $\pm i\omega_{\mathrm{UO}}$, corresponding to Matsubara frequencies arising from the undamped spectral component, which sum to the total undamped contribution. These modes correspond to coherent, undamped oscillations in the bath coordinate, which persist indefinitely and oscillate between ± 0.002. We note that there is still a small amount of growth, justified in terms of hierarchy stability in the supplementary material, which is magnified because there is no other bath from which energy and information can be transferred. This reflects the fundamentally energy-conserving nature of the undamped mode. Despite being part of an open system, the underdamped bath and system molecule effectively forms a closed system where energy and information is continually exchanging between the two without any net loss, as demonstrated by the dissipative $\mathrm{Y}^{(1)}$ measure which is symmetric about the x-axis .

The middle panels display the response of the overdamped bath component. The single bath LD model (middle right) shows pure decay of $\mathrm{X}^{(1)}$, and zero $\mathrm{Y}^{(1)}$ consistent with the lack of internal coherence or oscillatory structure. That is, the bath acts as a simple sink, rapidly losing memory of the system through monotonic loss of information, tending towards the equilibrium configuration. The projected LD component from the LDUO model (middle left) behaves similarly, although modified slightly by its indirect coupling to the UO component. Crucially, there is now a non-zero $\mathrm{Y}^{(1)}$ component which appears because of the system-bath-system coupling that is present in the LDUO model. Additionally, these behaviors underscore the difference between dissipative and conservative dynamics: the LD component loses memory and this facilitates equilibration (reaching a well defined plateau), while the UO component strongly retains memory. Interestingly, this appears to be amplified in the case

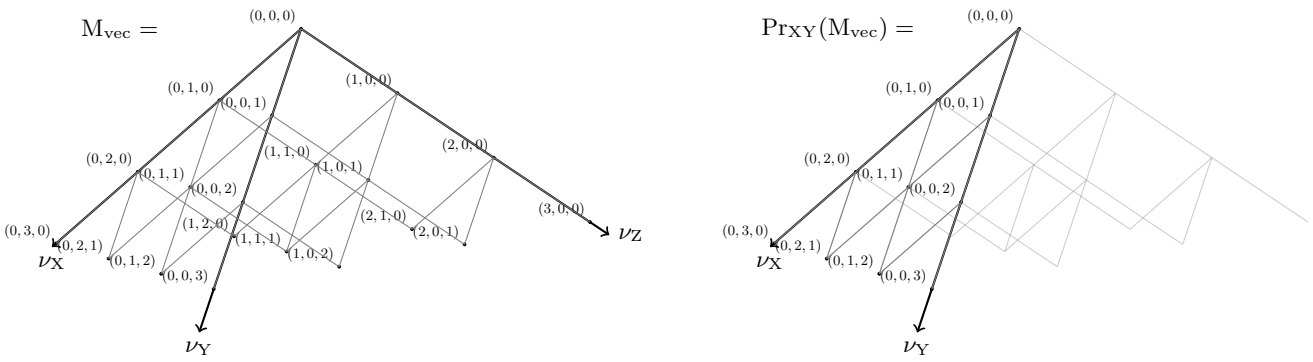

FIG. 4: A schematic of taking the projection onto the XY plane constituent of the collective bath mode resulting in the removal of the ν_Z Matsubara dimension from a generalised, 3D, hierarchy. Each dimension of this pyramid originates from a single spectral density. This schematic is for visualisation and typical, real, hierarchies can contain many more dimensions than three.

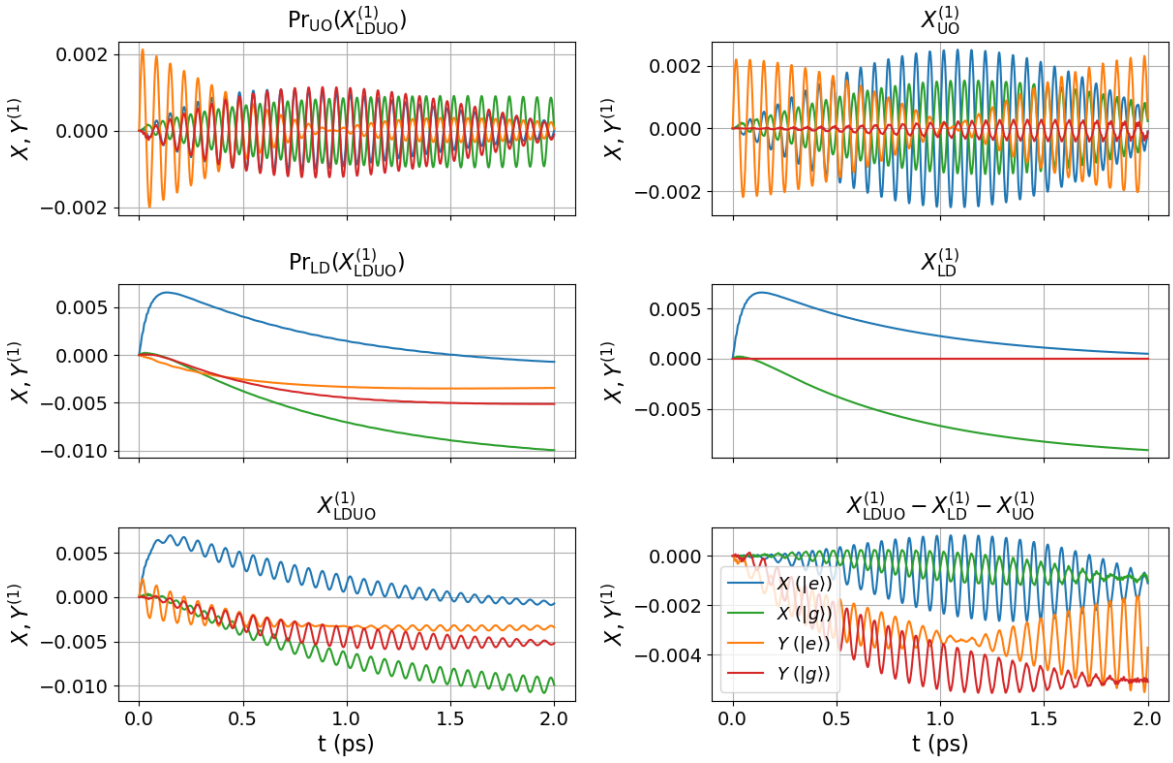

FIG. 5: Tier 1 expectation values. Column 1, the bath coordinate of the full LDUO, projected onto the UO plane, projected onto the LD plane, or unaltered. Column 2, the bath coordinate of the UO, the LD, and the difference between the full bath coordinate and the sum of its parts.

of the LDUO, where the baths are indirectly coupled via the system.

The bath coordinate of the full LDUO model (bottom left) reveals a hybrid picture, where the bath coordinate contains both persistent oscillations and decaying components. To test that we are definitely seeing information exchange between the baths, the bottom right panel shows a difference plot for $\mathrm{X}^{(1)}$ and $\mathrm{Y}^{(1)}$, with contributions from the individual baths subtracted from that of the total LDUO. We see that the latter is not simply the sum of UO and LD parts. That is, nontrivial residuals remain due to interaction between the coherent and dissipative channels. It is therefore clear that strong bath-system-bath coupling occurs within the LDUO model.

Figures 7 and 8 show the results for a decomposition of the bath coordinate expectation values as a second order moment $\mathrm{X}^{(2)}(t)$ and $\mathrm{Y}^{(2)}(t)$. These results can be interpreted in terms of two phonon processes as variances of the bath coordinate from the total Matsubara modes present in A_0.

In the top left panel of figure 7, the projected undamped component of the full LDUO system, shows a strong oscillation for both the fluctuating and dissipative components $\mathrm{X}^{(2)}$ and $\mathrm{Y}^{(2)}$. The increased amplitude of the UO contributions with respect to their projections, and the broken symmetry of $\mathrm{Y}^{(2)}$ around the x-axis reflects the coherent build-up of information in the undamped subspace of the hierarchy being lost into the LD bath which is accompanied by a decrease in the effective bath coordinate in the LD subspace of the hierarchy. We hypothesise that this is due to a net positive information flux returning to the system, due to strong non-Markovian effects. Since no dissipation pathway exists for the pure undamped mode, the displacement of the bath's effective coordinate increases over time, as a result of the bath-system-bath coupling. In contrast, the top right panel shows the single bath UO trajectory. Unlike the projected LDUO component, the amplitude of the both fluctuation and dissipation components ($\mathrm{X}^{(2)}$, $\mathrm{Y}^{(2)}$) remain bounded for the ground and excited state populations with the isolated bath coordinate coherently oscillating under purely imaginary Matsubara-like frequencies $\pm i\omega_{\mathrm{UO}}$. This suggests that the bath-system-bath coupling in the total LDUO dynamics suppresses this symmetric growth in amplitude of $\mathrm{X}^{(2)}(t)$ and $\mathrm{Y}^{(2)}$.

Figure 8 shows individual contributions to the total $\mathrm{X}^{(2)}$ and $\mathrm{Y}^{(2)}$ signal (that is each of the terms in equations (75) and (77)). The top two subplots (UO_0 and UO_1) are identical in shape to each other, but with a relative phase delay, which is consistent with dynamics arising from terms involving the two Matsubara coefficients, c_k, in equation (35), and their associated complex conjugate frequencies, γ_k. The bottom two subplots show the tier 0 component of the static time correlator (left) and the doubly excited mode configuration. In both cases a plateau forms as the system reaches global equilibrium, and in the UO cross signal there is also a strong oscillatory component from the undamped modes. It is clear from these results that the dominant contributions are those which arise from the tier zero contribution, which are of the order of the $\hbar\omega\lambda$, which is consistent with previous results in Zhu et al. 43.

We now turn our attention to the LD component, and refer back to the middle panels of figure 7. The projected LD component from the two bath model (middle left panel) exhibits very low intensity oscillations at the undamped mode frequency giving rise to a plateauing decay to the equilibrium configuration, for both the excited and ground states. This is in contrast to the the middle right panel, where there are no direct contributions from the undamped modes. While both the excited and ground states still decay to the same approximate equilibrium value there is a larger increase at early time, due to the absence of the dissipative, $\mathrm{Y}^{(2)}$, signals . This is because there are no oscillatory features due to the undamped modes present within the signals, and consequently there is much more symmetric variance between the populations. This is consistent with a bath that acts purely as a memoryless sink as the system continuously loses information to the bath. These panels, once again highlight the strong sensitivity to bath coordinate displacements introduced via indirect system-bath-system coupling in the LDUO model.

In the bottom left panel, the full $\mathrm{X}^{(2)}$ and $\mathrm{Y}^{(2)}$ from the LDUO model shows that both fluctuation and dissipation components converge to an equilibrium over time, but modulated by long-lived oscillations suggesting strong population-dependent dressing of the bath with vibrational and thermal contributions. To examine whether the LDUO result can be decomposed additively, the bottom right panel plots the difference $\mathrm{X}^{(2)}_{\mathrm{LDUO}} - \mathrm{X}^{(2)}_{\mathrm{LD}} - \mathrm{X}^{(2)}_{\mathrm{UO}}$ and $\mathrm{Y}^{(2)}_{\mathrm{LDUO}} - \mathrm{Y}^{(2)}_{\mathrm{LD}} - \mathrm{Y}^{(2)}_{\mathrm{UO}}$. Substantial non-zero residuals remain, confirming that the LDUO result is not simply the sum of independent underdamped and overdamped baths. This confirms the presence of significant bath-bath correlations mediated via the system, and highlights that the fluctuation dynamics of the environment in LDUO cannot be interpreted as a linear superposition of simpler baths.

VI. CONCLUSION

The derivation of our LDUO model was motivated by the desire to remove superfluous canonical damping from our BVM model. We indeed show that we get qualitatively similar spectra to those of the uHEOM BVM while dramatically improving the computational efficiency, reducing the CPU time by 99.4%, or more, in the weak coupling case.

Perhaps more interestingly, the development of this model has also demonstrated that there is a strong bath-system-bath coupling present in two bath models which is not present in single bath alternatives, via first and second order bath coordinate expectation values. The bath-system-bath coupling, inherent in this model leads to in-

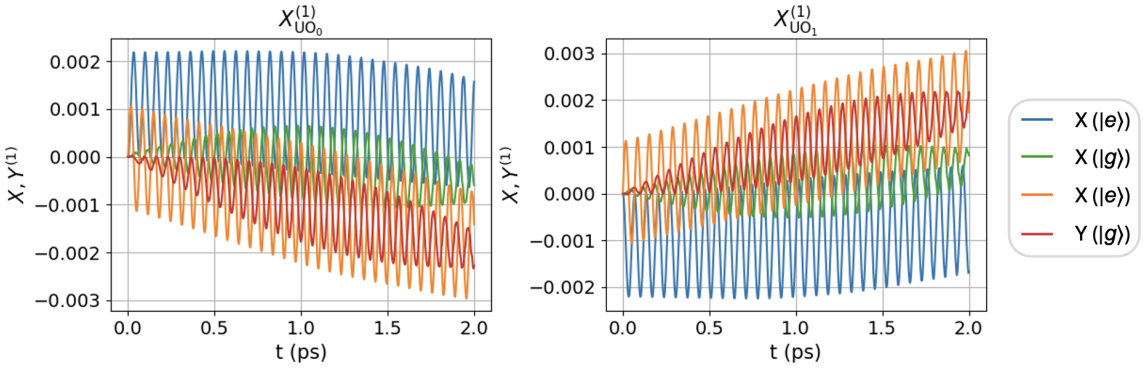

FIG. 6: Tier 1 expectation values. The bath coordinate of the UO, further decomposed into its UO_0 and UO_1 mode components.

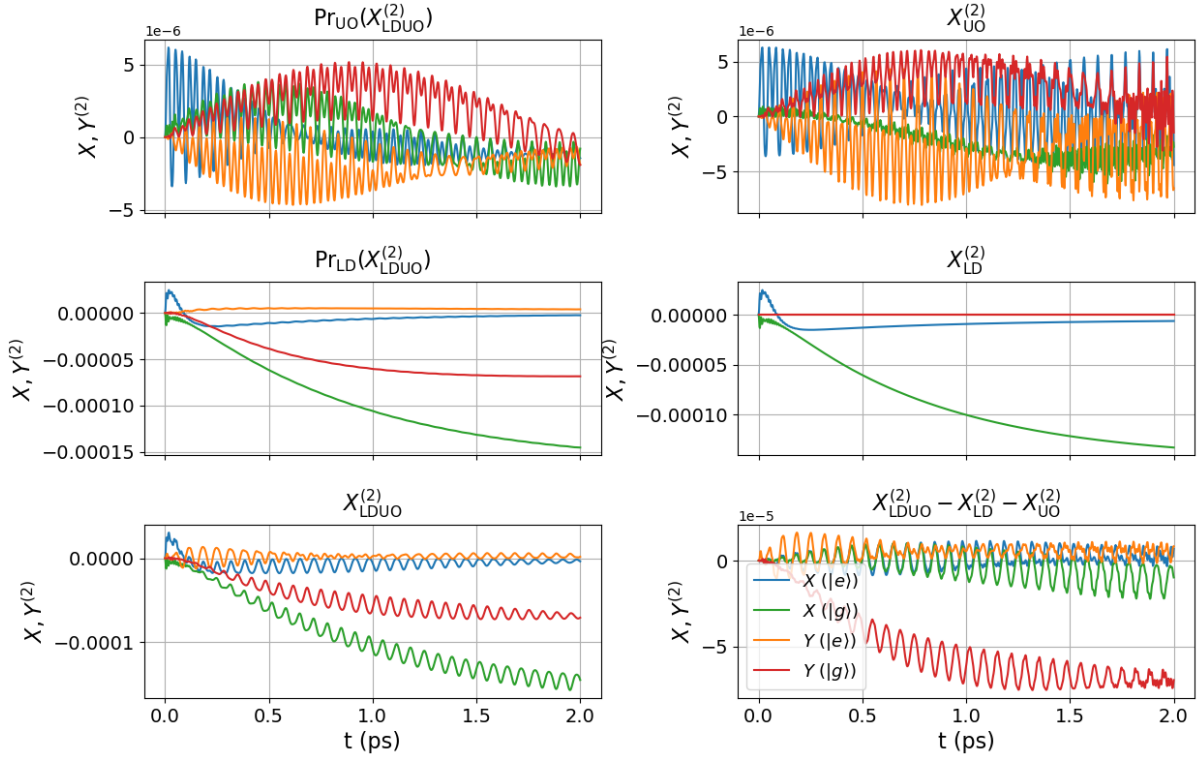

FIG. 7: Tier 2 expectation values. Column 1, the bath coordinate of the full LDUO, projected onto the UO plane, projected onto the LD plane, or unaltered. Column 2, the bath coordinate of the UO, the LD, and the difference between the full bath coordinate and the sum of its parts.

direct communication (information transfer) between the baths. Practically, such nonlinear couplings can have a profound impact on system dynamics: for example in a system with electronic dephasing and vibrational relaxation baths the bath-system-bath coupling induces nontrivial electronic-vibrational coupling from the dephasing and vibrational processes which would be absent in a single bath approach. Future work could look at the effect of combining baths via tensor products on bath dynamics.

VII. SUPPLEMENTARY MATERIAL

The supplementary material includes an outline of a comparative, well studied, overdamped version of the HEOM which is close in structure to the derived LDUO HEOM. This is used to benchmark the LDUO variant in the paper. In addition, two further sections are included, one presenting convergence tests for the presented results, and another showing numerical stability tests of both hierarchies.

ACKNOWLEDGMENTS

The research presented in this paper was carried out on the High Performance Computing Cluster supported by the Research and Specialist Computing Support service at the University of East Anglia. B.S.H thanks the Faculty of Science, University of East Anglia for studentship funding. G.A.J. and D.G. acknowledge support from the Engineering and Physical Sciences Research Council under Awards No. EP/V00817X/1. B.S.H thanks Dr. Joachim Seibt for valuable discussion on the HEOM.

CONFLICTS OF INTEREST

The authors have no conflicts of interest to disclose.

DATA AVAILABILITY

The data that support the findings of this contribution are available from the corresponding authors upon reasonable request.

REFERENCES

[1]K. Kuroiwa and H. Yamasaki, Physical Review A **104**, L020401 (2021).
[2]G. D. Berk, S. Milz, F. A. Pollock, and K. Modi, npj Quantum Information **9**, 104 (2023).
[3]S. Koyanagi and Y. Tanimura, J. Chem. Phys. **161**, 112501 (2024).
[4]S. Koyanagi and Y. Tanimura, J. Chem. Phys. **161**, 162501 (2024).
[5]G. Pleasance and F. Petruccione, New J. Phys. **26**, 073025 (2024).
[6]H. M. Friedman, B. K. Agarwalla, and D. Segal, New J. Phys. **20**, 083026 (2018).
[7]F. Altıntaş, Eur. Phys. J. Plus **140**, 621 (2025).
[8]A. Kato and Y. Tanimura, J. Chem. Phys. **145**, 224105 (2016).
[9]M. Kilgour and D. Segal, Phys. Rev. E **98**, 012117 (2018).
[10]L. Song and Q. Shi, Phys. Rev. B **95**, 064308 (2017).
[11]Y. Tanimura, J. Chem. Phys. **153** (2020), 10.1063/5.0011599.
[12]Y. Tanimura, Phys. Rev. A **41**, 6676 (1990).
[13]Y. J. Yan, J. Jin, R. X. Xu, and X. Zheng, Front. Phys. **11** (2016), 10.1007/s11467-016-0513-5.
[14]T. Ikeda and G. D. Scholes, J. Chem. Phys. **152**, 204101 (2020), arXiv:2003.06134.
[15]J. J. Ding, R. X. Xu, and Y. Yan, J. Chem. Phys. **136** (2012), 10.1063/1.4724193.
[16]W. Wu, Phys. Rev. A **98**, 1 (2018), arXiv:1709.04649.
[17]J. Seibt and O. Kühn, J. Chem. Phys. **153** (2020), 10.1063/5.0027373.
[18]B. S. Humphries, *Impact of a Movable System-Bath Boundary on Photon and Phonon Correlations and Quantum Information in Hierarchically Modelled Open Systems.*, Ph.D. thesis, The University of East Anglia (2024).
[19]J. Iles-Smith, N. Lambert, and A. Nazir, Phys. Rev. A **90**, 032114 (2014).
[20]H. Maguire, J. Iles-Smith, and A. Nazir, Phys. Rev. Lett. **123**, 093601 (2019).
[21]C. McConnell and A. Nazir, J. Chem. Phys. **151** (2019), 10.1063/1.5095838.
[22]B. S. Humphries, D. Green, and G. A. Jones, J. Chem. Phys. **156**, 1 (2022).
[23]Y. Tanimura, J. Chem. Phys. **137** (2012), 10.1063/1.4766931.
[24]Y. Tanimura, J. Phys. Soc. Japan **75**, 082001 (2006).
[25]Y. Tanimura, J. Chem. Phys. **141** (2014), 10.1063/1.4890441.
[26]H. Liu, L. Zhu, S. Bai, and Q. Shi, J. Chem. Phys. **140**, 134106 (2014).
[27]Y. Yan, T. Xing, and Q. Shi, J. Chem. Phys. **153**, 204109 (2020).
[28]I. S. Dunn, R. Tempelaar, and D. R. Reichman, J. Chem. Phys. **150** (2019), 10.1063/1.5092616.
[29]A. Garg, J. N. Onuchic, and V. Ambegaokar, J. Chem. Phys. **83**, 4491 (1985).
[30]Y. Lai and E. Geva, J. Chem. Phys. **155** (2021), 10.1063/5.0069313.
[31]D. Green, B. S. Humphries, A. G. Dijkstra, and G. A. Jones, J. Chem. Phys. **151**, 174112 (2019).
[32]Y. Tanimura, J. Chem. Phys. **153**, 020901 (2020), arXiv:arXiv:2006.05501v2.
[33]A. Caldeira and A. Leggett, Phys. A Stat. Mech. its Appl. **121**, 587 (1983).
[34]A. Caldeira and A. Leggett, Phys. Rev. Lett. **49**, 1545 (1981).
[35]R. Feynman and F. Vernon, Ann. Phys. (N. Y). **24**, 118 (1963), arXiv:0306052 [gr-qc].
[36]R. P. Feynman, A. R. Hibbs, and G. H. Weiss, " Quantum Mechanics and Path Integrals ," (1966).
[37]Y. Tanimura and R. Kubo, J. Phys. Soc. Japan **58**, 101 (1989).
[38]J. Seibt and T. Mančal, Chem. Phys. **515**, 129 (2018), arXiv:1807.07475.
[39]J. Seibt and T. Mančal, Chem. Phys. **515**, 129 (2018).
[40]A. Ishizaki and Y. Tanimura, J. Phys. Soc. Japan **74**, 3131 (2005).
[41]A. G. Dijkstra and V. I. Prokhorenko, J. Chem. Phys. **147**, 064102 (2017).
[42]M. Tanaka and Y. Tanimura, J. Phys. Soc. Japan **78**, 073802 (2009).
[43]L. Zhu, H. Liu, W. Xie, and Q. Shi, J. Chem. Phys. **137** (2012), 10.1063/1.4766358.
[44]Q. Shi, L. Chen, G. Nan, R. Xu, and Y. Yan, J. Chem. Phys. **130** (2009), 10.1063/1.3125003.
[45]M. Noack, A. Reinefeld, T. Kramer, and T. Steinke, Proc. - 2018 IEEE 32nd Int. Parallel Distrib. Process. Symp. Work. IPDPSW

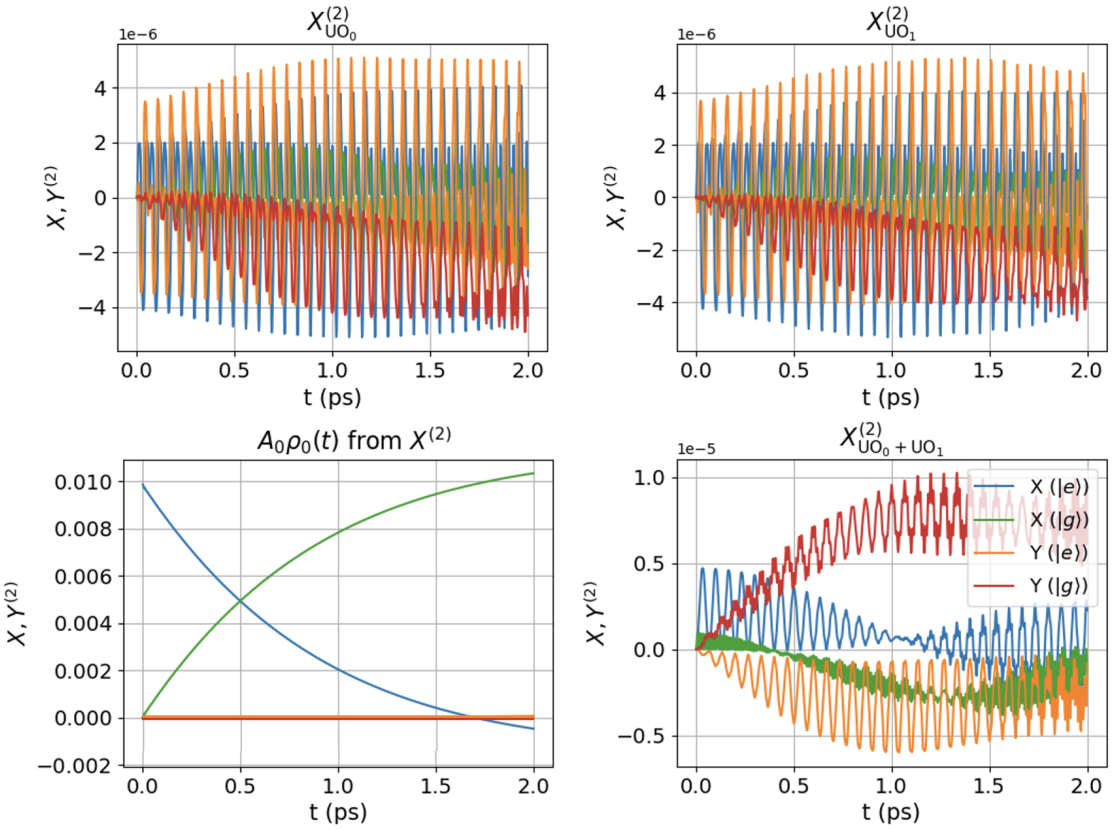

FIG. 8: Components of the tier 2 expectation values. Column 1, the bath coordinate of the UO_0 mode and tier 0 portions. Column 2, the bath coordinate of the UO_1 mode, and the doubly coupled UO_0 and UO_1 portions.

2018 , 947 (2018).
[46]U. Deker and F. Haake, Phys. Rev. A **11**, 2043 (1975).
[47]G. C. Wick, Phys. Rev. **80**, 268 (1950).
[48]R. Hübener, A. Mari, and J. Eisert, Phys. Rev. Lett. **110**, 040401 (2013).
[49]R. Kubo, Reports on Progress in Physics **29**, 255 (1966).